INFLUENCE OF FLY ASH ADDED TO A CERAMIC BODY ON ITS THERMOPHYSICAL PROPERTIES

by

Jozef KOVAC[a], Anton TRNIK[a,b,*], Igor MEDVED[a,b]*, Igor STUBNA[a], and Libor VOZAR[a]

[a] Department of Physics, Faculty of Natural Sciences, Constantine the Philosopher University, Nitra, Slovakia
[b] Department of Materials Engineering and Chemistry, Faculty of Civil Engineering, Czech Technical University, Prague, Czech Republic

Original scientific paper
DOI: 10.2298/TSCI130911077K

We study thermal expansion, mass changes, heat capacity, and thermal diffusivity and conductivity for a ceramic body with 20 mass% and without fly ash content, using the thermodilatometric analysis, thermogravimetric analysis, differential thermal analysis, differential scanning calorimetry, and flash method. The measurements were performed: (a) for green samples either isothermally or by a linear heating up to a temperature 600 °C, 1050 °C, or 1100 °C, depending on the measurement method; (b) at the room temperature for samples preheated at 100 °C, 200 °C, ..., 1100 °C. In case (a) addition of fly ash changes the final contraction only above ~900 °C, while the thermal properties remain almost unchanged. In case (b) the final contraction of samples at 1100 °C is the same. The thermal diffusivity is nearly identical up to 700 °C, and fly ash causes the diffusivity to stay almost constant up to 1000 °C.

Key words: *thermal contraction, thermal diffusivity, ceramics, fly ash*

Introduction

The use of waste materials in the production of various commodities has become an important issue due to its potential to the environment as well as to lower production costs. In order to optimize the content of waste materials so that the final products exhibit the needed physical and chemical properties, detailed understanding of the influence of the waste materials is critical.

Building ceramics are usually made from a raw mixture with a high content of kaolinitic and/or illitic clay. These materials exhibit changes in their physical properties during firing due to dehydration at lower temperatures, phase changes during dehydroxylation, high-temperature reactions, and sintering [1-3]. Quartz, feldspar, and calcite are very often the natural components of ceramic clays. These minerals also change their composition and structure in the temperature range which is commonly used in building ceramic industry.

In the past decades, the use of various kinds of waste in ceramic industry has occurred. For example, organic waste has been successfully used for manufacturing porous bricks with a low thermal conductivity [4-6]. A calcite waste, as an admixture in kaolinitic clay, has been used as a flux, decreasing the irreversible contraction during firing of the bricks

* Corresponding author; e-mail: atrnik@ukf.sk

and tiles [7-9]. Fly ash, the waste which comes from burning of coal in thermal power stations, is an alternative source of minerals which are usually present in the composition of building ceramics. There are similarities between fly ash and traditional minerals, such as their composition and fine particles. From the viewpoint of the chemical composition, fly ash is a mixture of SiO_2, Al_2O_3, Na_2O, Fe_2O_3, CaO, and TiO_2, and some other minerals [10, 11]. Fly ash in a raw mixture leads to an improvement of mechanical properties of the fired ceramics [10, 12, 13]. The mechanical strength of the ceramic tiles with fly ash as a raw material fulfills the necessary requirements [11, 14].

The objective of this paper is a complex experimental study of thermophysical properties of ceramic samples with 20 mass% of fly ash and compared them to those of the same ceramics without any fly ash content. To this end, we applied the thermodilatometric (TDA), thermogravimetric (TGA), differential thermal analyses (DTA), differential scanning calorimetry (DSC), and standard flash method. In the section *Experimental* we describe the studied samples and their preparation and composition. We also briefly describe the employed experimental methods.

Experimental

Samples

We analyzed two types of ceramic samples. One (denoted here as *F*) contained 20 mass% of fly ash, while the other one (denoted as *R*) was a reference sample with no fly ash. The compositions of samples *F* and *R* are given in tab. 1. Both samples contained 60 mass% of clay B1 (supplied by LB-Minerals Ltd.), the remaining part was a filler (clay B1 fired at 1000 °C with a soaking time 90 min at the highest temperature). Clay B1 consisted of kaolinite (65 mass%), illite (25 mass%), muscovite (3 mass%), 5 mass% of free quartz, and 2 mass% of undefined filler [15]. The chemical compositions of clay B1 and fly ash are given in tab. 2. The fly ash was provided by the electric power plant in Hodonin, Czech Republic.

Table 1. Composition of the samples [mass%]

Sample	Clay	Filler	Fly ash
F	60	40	–
R	60	20	20

Table 2. Chemical composition of clay B1 and fly ash in mass%

	SiO_2	Al_2O_3	Fe_2O_3	TiO_2	CaO	MgO	K_2O	Na_2O	Sulphates	LOI
Clay B1	48.6	33.8	2.6	0.8	0.28	0.36	1.98	0.10	–	11.3
Fly ash	28.6	16.4	6.9	0.5	32.7	4.3	0.6	0.9	4.0	5.1

To prepare the samples, we ground fired clay B1 and fly ash, sieved them, and then mixed them with clay B1 and water to obtain a plastic mass with a water content ~25 mass%. Subsequently, we used a laboratory extruder to prepare cylindrical samples with diameters 11.5 mm. These were subject to open air free drying after which the samples contained ~2 mass% of physically bound water.

Measurement methods

We determined the relative expansion in dependence on the temperature using the TDA. Namely, we used a horizontal push-rod dilatometer designed and constructed in our laboratory [16]. The dimensions of the cylindrical samples used in the measurements were

∅11 × 40 mm. Using the experimental data on the relative expansion, the linear thermal expansion coefficient (LTEC) was calculated as the derivative of the expansion with respect to the thermodynamic temperature [17-19].

The mass changes in a controlled temperature regime were obtained from the TGA. The analysis was performed by a simultaneous TGA/DTA analyzer Derivatograph 1000 (Hungary) [20]. A reference compact sample for DTA with approximately the same size and weight as the measured green ceramic sample was made from pressed Al_2O_3 powder. The dimensions of the samples were ∅11 × 20 mm.

Using the experimental results on the thermal strain ($\Delta l/l_0$) and the relative mass changes ($\Delta m/m_0$), the corresponding density was calculated:

$$\rho = \rho_0 \frac{1+\Delta m/m_0}{1+3\Delta l/l_0} \tag{1}$$

where ρ_0 is the initial density.

The specific heat capacity, c_p, was measured by the DSC. The DSC is based on the measurement of the heat flux difference between a sample and a reference sample while they are subject to a controlled temperature regime (heated, cooled, or held at a constant temperature). Comparing the measured heat flux with that of sapphire (which usually acts as a reference and whose specific heat capacity is known), the specific heat capacity of the studied sample is determined. In our measurements we used the DSC Mettler Toledo 822e and powder samples.

To measure the thermal diffusivity, a, we used the standard flash method [21]. This method is based on the measurement of a thermal response on one side of a material due to heating of its opposite side by a short heat-pulse (in our case the pulse was generated by a xenon flash lamp) [22]. In fact, using differentially connected thermocouples, a temperature difference between the investigated and reference samples is measured (the reference sample is not exposed to the pulse). The measurement apparatus is placed in a furnace whose temperature is regulated by an adjustable voltage source. The dimensions of the samples were ∅11 × 1 mm.

The thermal conductivity, λ, was subsequently determined as:

$$\lambda = a\ \rho\ c_p \tag{2}$$

using the already measured values of ρ and c_p.

The uncertainty in our measurements were obtained in a standard way as a combination of errors of type A and B [23, 24]. Namely, the relative uncertainty was 0.6% for the TDA measurements [16], 0.3% for the TGA measurements [20], 3.2% for the heat capacity measurements [25], and 5.3% for the thermal diffusivity measurements [25]. We carried out a similar error analysis for the measurement of Young's modulus and the mechanical strength [26, 27].

Two types of measurements were performed. In one type we used the green samples that were studied from room temperature up to a temperature, T_0, either isothermally with a ~50 °C step (in the case of the thermal diffusivity) or by a linear heating with rate 5 °C min^{-1} (for the remaining quantities). The maximal temperature was chosen as 600 °C in the measurement of the specific heat capacity and thermal diffusivity, 1050 °C for the mass changes and DTA, and 1100 °C for the thermal strain. In the other type we measured the samples at the room temperature that were preheated at 100 °C, 200 °C, ..., 1100 °C with soaking time 1 min. The temperature 1100 °C was chosen for both types because it is the presumptive highest firing temperature used in industry for clay tiles. The meaning of these two types of measurements is clear: while the former allows one to study changes of the considered properties during heat

treatment, the latter provides the knowledge on the materials properties after firing at a given temperature and, thus, helps to design materials for a specific application.

Results and discussion

Both the structure and composition of the studied samples change during heating. These changes determine all physical properties of the samples, including thermophysical properties. In general, the results of the DTA reveal the processes in the samples which are linked with the consumption and release of heat and which are represented as maxima and minima in the DTA curve, respectively. Our DTA results (fig. 1) suggest that the DTA curve may be divided into five parts.

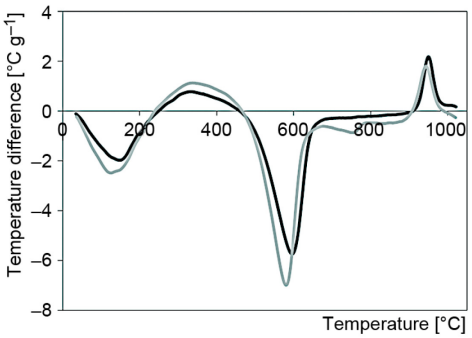

Figure 1. The DTA of ceramic samples *R* (black line) and *F* (gray line)

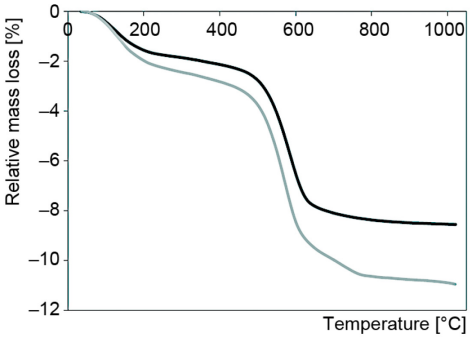

Figure 2. Relative mass loss of ceramic samples *R* (black line) and *F* (gray line)

– An endothermic peak in the temperature range 25-250 °C represents the liberation of physically bound water from the pores and surfaces of the crystals in the samples. This process is reflected by a relatively large decrease in the mass by ~2% and ~2.5% for sample *R* and *F*, respectively (fig. 2). Due to this difference, in the TDA curve a contraction is registered for sample *F*, while an expansion occurs for sample *R* in this temperature interval (fig. 3). Both the contraction and mass loss lead to a decrease in the density (fig. 4). The liberation of physically bounded water from the pores and crystals surfaces makes the contacts between crystals stronger [9].
– In the temperature range 250-450 °C an exothermic peak is visible. It is related to clay B1 and, consequently, to the studied samples containing a small amount of organic impurities. This was confirmed by the evolved gas analysis which recorded CO_2 during heating in 300-500 °C [15]. The process leads to a small decrease of the sample mass.
– The second endothermic peak in the DTA curve (fig. 1) corresponds to the dehydroxylation of kaolinite and illite which begins at ~450 °C and finishes at ~650 °C for the studied samples. The dehydroxylation is accompanied by shrinkage of the samples as well as a mass loss [28-33]. However, the samples contained also calcite (as a part of fly ash), quartz, and fired clay B1 which do not undergo dehydroxylation. Thus, the total thermal expansion is a sum of the contraction of kaolinite (which changes into metakaolinite) and the expansion of calcite, quartz, and fired clay B1.
– The third endothermic peak represents the decomposition of calcite (contained in fly ash) given as $CaCO_3 \rightarrow CaO + CO_2$ which runs in the temperature interval 700-900 °C and is accompanied by the mass loss of calcite (44 mass%) [34]. This endothermic reaction begins with the formation of a mesoporous structure of CaO nanocrystals (~5 nm in thickness) and

pores (~250 nm in diameter) in the places where the crystals $CaCO_3$ were initially presented [35]. The endothermic essence of this reaction and mass loss are visualized in figs. 1 and 2. In the temperature interval 450-900 °C the dimensions of the sample change only by up to 0.15%, while the relative mass loss is significantly higher (up to 11%). Consequently, the density decreases until the decomposition of calcite is terminated at ~800 °C (fig. 4).

– The second exothermic reaction occurs at temperature ~950 °C and can be considered as the collapse of the dehydroxylated phyllosilicate structures, which is associated with an increase of its volume. It causes a slowdown in the contraction (fig. 3) and a disruption in the density increase (fig. 4) of both samples *R* and *F*.

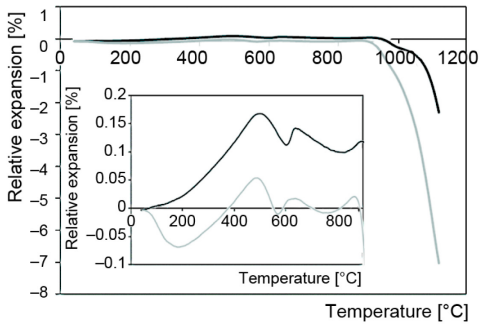

Figure 3. Relative expansion of ceramic samples *R* (black line) and *F* (gray line)

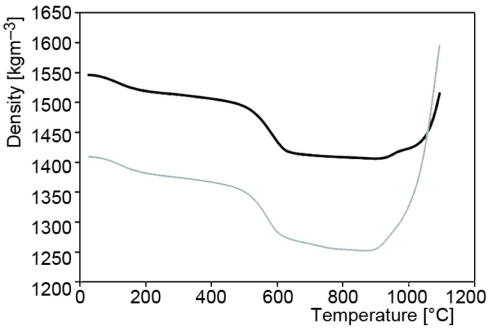

Figure 4. Density of ceramic samples *R* (black line) and *F* (gray line)

From the comparison of the results of the DTA analysis of samples *R* and *F* (fig. 1) we may conclude that the curve profiles are almost identical up to the temperature ~650 °C. The reason is that the samples contained the same mass% of clay B1 and had approximately the same moisture at the beginning (as follows from the mass loss shown in fig. 2). Above the temperature ~650 °C the curve profiles are different because of calcite contained in fly ash and, thus, in sample *F*. This is justified by the results of the mass loss (fig. 2). Indeed, sample *R* (not containing fly ash) lost ~8% of its mass, while sample *F* lost ~11 mass%. After the decomposition of calcite at ~800 °C no mass changes are detected any longer. At ~950 °C the exothermic reaction of the collapse of the dehydroxylated phyllosilicate structures occurs in samples *R* and *F*.

Comparing the relative expansion of the two samples *R* and *F* (fig. 3), we observe that, similarly to the mass change, there are very small differences up to the temperature ~850 °C. After the calcite decomposition, a small contraction occurs for sample *F* it is ~1%. Interestingly, the final contraction of the samples (at 1100 °C) is larger for sample *F* (with fly ash), attaining ~7%, while it is ~2.3% for sample *R*. These length changes are clearly visible in fig. 5 where the thermal expansion coefficients of samples *R* and *F* are shown.

After an analysis of the basic properties of the studied samples, we shall now analyze our results concerning the thermal conductivity and diffusivity and the specific heat capacity. Our experimental data on the thermal diffusivity in the temperature range 25-600 °C are given in fig. 6. This interval was chosen due to the limitations of our measurement apparatus. They allow us to conclude whether the presence of fly ash affects the thermal diffusivity in this range of temperatures. The data show that *a* decreases with temperature for both samples *F* and *R*. Moreover, samples *R* and *F* have almost the same *a* in the temperature ranges 100-300 °C and 500-600 °C. However, in the interval 25-100 °C sample *R* has a higher *a* than sample *F*, whereas in the interval 300-500 °C sample *F* has a higher *a* than sample *R*.

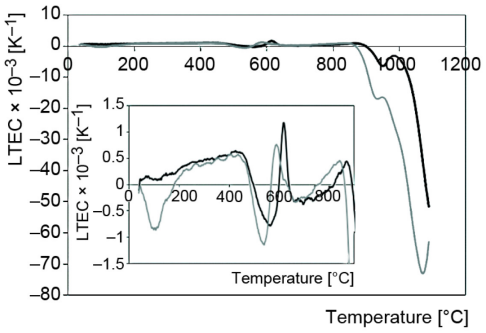

Figure 5. Linear thermal expansion coefficient of ceramic samples *R* (black line) and *F* (gray line)

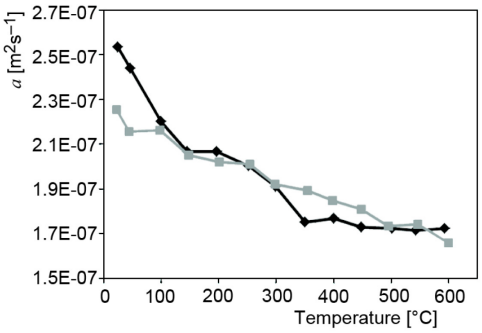

Figure 6. Thermal diffusivity of ceramic samples *R* (black line) and *F* (gray line)

Besides the thermal diffusivity, in the same temperature interval we also investigated the specific heat capacity of the samples (fig. 7). Similarly to a, these results imply that the effect of fly ash on c_p is very little. In both samples R and F a slight increase in c_p occurs due to the liberation of physically bounded water in the temperature range 25-150 °C, followed by a slow decrease until the beginning of dehydroxylation at ~450 °C. During dehydroxylation a rather sharp peak in c_p (associated with the corresponding first-order phase transition) is observed. The peak ends when dehydroxylation is completed.

Finally, using the experimental data on the thermal diffusivity and the specific heat capacity c_p, we evaluated the thermal conductivity, λ, of the studied samples, using eq. (2) (fig. 8). The profiles of thus obtained curves are similar to those for c_p. In the investigated temperature range the effect of fly ash on λ is practically negligible.

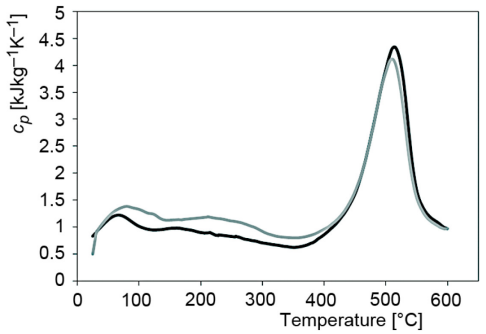

Figure 7. Specific heat capacity of ceramic samples *R* (black line) and *F* (gray line)

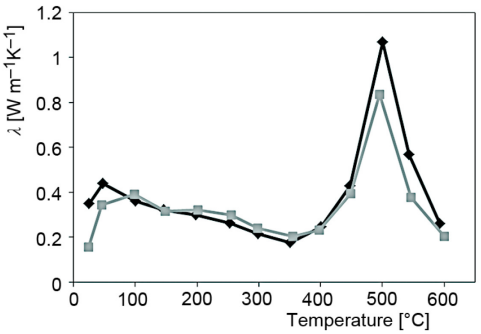

Figure 8. Thermal conductivity of ceramic samples *R* (black line) and *F* (gray line)

After investigating the properties of the samples during firing, we studied the properties of samples preheated at various temperatures ranging up to 1100 °C. The mass changes of thus preheated samples are shown in fig. 9. They are almost identical to those in fig. 2 obtained for samples that were not preheated. We may observe the liberation of physically bounded water, dehydroxylation, and calcite decomposition.

The results on the thermal expansion (fig. 10) show that the expansion of sample R is almost constant up to the temperature ~800 °C, whereas the expansion of sample F decreases up to the temperature ~500 °C, reaching –0.24%, and then slightly increases up to

~800 °C. From the temperature ~800 °C the thermal expansion of sample *R* slowly decreases and after 900 °C the contraction starts to increase rapidly. The different results were obtained for sample *F* containing fly ash. Its thermal expansion sharply decreases till 1100 °C. Finally, at the temperature ~1100 °C we observe that the expansion of samples *F* and *R* is nearly the same, reaching ~9%. Therefore, we may conclude that fly ash has no impact on the final contraction of samples.

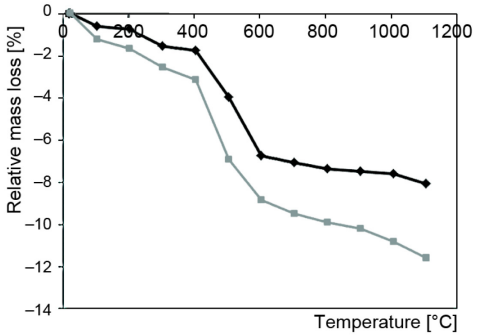

Figure 9. Relative mass loss of ceramic samples *R* (black line) and *F* (gray line) after firing

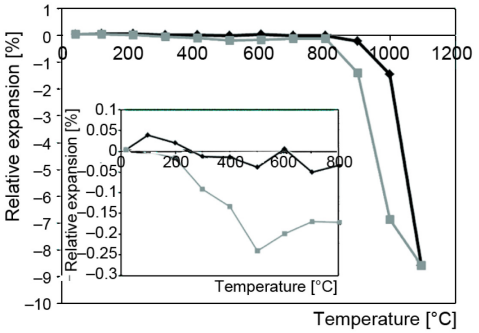

Figure 10. Relative expansion of ceramic samples *R* (black line) and *F* (gray line) after firing

Using the measured values of the sample dimensions and masses, we calculated their density (fig. 11). Its value was 1540 kgm^{-3} for green sample *R* and 1400 kgm^{-3} for green sample *F*. With an increasing firing temperature the density of the samples slowly decreased up to ~400 °C. Then a larger decrease occurred due to dehydroxylation. After dehydroxylation terminated, the density of samples *F* and *R* was almost constant. From 900 °C a rapid increase in the density of sample *R* takes places, reaching ~2120 kgm^{-3} for the temperature 1100 °C. On the other hand, the density of sample *F* slightly grows between 800 °C and 900 °C and then there is a rapid increase up to ~1900 kgm^{-3}.

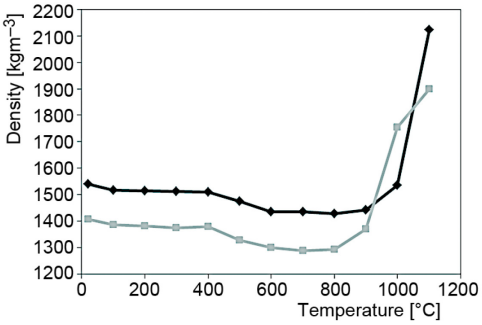

Figure 11. Density of ceramic samples *R* (black line) and *F* (gray line) after firing

Finally, we measured the dependence of the thermal diffusivity on the firing temperature up to 1100 °C (fig. 12). The data shows that the dependence is almost identical for both samples *F* and *R* up to the temperature 700 °C. Rather interesting differences occur from the temperature 700 °C. The thermal diffusivity of sample *R* has a slight change at 700 °C a subsequently increases proportionally with the firing temperatures of 800 °C and 900 °C, reaching ~4.8 m^{2}s^{-1}. This value of *a* is unchanged for the temperature 1000 °C. However, increasing the firing temperature to 1100 °C causes another large increase in *a* to ~7.2 m^{2}s^{-1}.

For sample *F* containing fly ash its thermal diffusivity at 700 °C slightly increases. With an increase of the firing temperature to 800 °C the thermal diffusivity of sample *F* decreases to almost the value for the firing temperature 600 °C. A further increase to 900 °C causes the thermal diffusivity to increase again, this time to ~2.2 m^{2}s^{-1}. The thermal diffu-

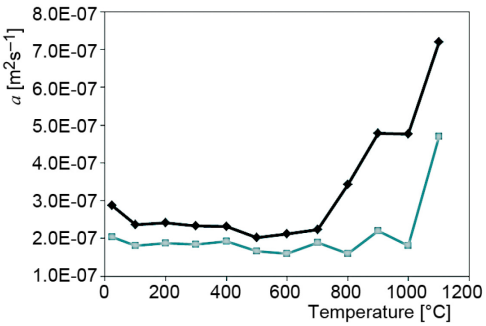

Figure 12. Thermal diffusivity of ceramic samples *R* (black line) and *F* (gray line) after firing

sivity of sample *F* exhibits a sudden change at 1000 °C, decreasing back to the value corresponding to 700 °C. In the end, at 1100 °C the thermal diffusivity of sample *F* rapidly increased to ~4.7 m^2s^{-1}, which is by about 1/3 less than for sample *R*.

Conclusions

We investigated thermophysical properties – the thermal expansion, mass changes, specific heat capacity, and thermal diffusivity and conductivity – for a ceramics with 20 mass% of fly ash and compared them to those of the same ceramics without any fly ash content. To this end, we applied the TDA, TGA, and DTA analyses, DSC, and flash method. Two types of measurements were performed: one was for green samples either isothermally with a 50 °C step or by a linear heating with rate 5 °C min^{-1} up to a temperature 600 °C, 1050 °C, or 1100 °C, depending on the measurement method; the other one was at room temperature for samples preheated at 100 °C, 200 °C, ..., 1100 °C.

For the former type we showed that the final contraction of the samples (at 1100 °C) was about three times larger for sample with fly ash. Moreover, addition of fly ash had practically no effect on the thermal diffusivity and conductivity and specific heat capacity.

For the latter type we found that the final contraction of samples at 1100 °C nearly did not change after addition of fly ash. Furthermore, the thermal diffusivity was also almost identical for firing temperatures up to 700 °C. However, 800-1000 °C addition of fly ash makes the diffusivity stay almost constant. An increase occurred only at 1100 °C, being just two thirds of the case when no fly ash is added.

Acknowledgments

This research was supported by the Czech Science Foundation, Project No. P105/12/G059 and by the grant VEGA 1/0162/15.

Nomenclature

a – thermal diffusivity, [m^2s^{-1}]
c_p – specific heat capacity, [$kJkg^{-1}K^{-1}$]
l_0 – initial length, [mm]
Δl – length change, [mm]
LTEC – linear thermal expansion coefficient, [K^{-1}]
m_0 – initial mass, [g]
Δm – mass change, [g]
T_0 – temperature, [°C]
R – reference sample with no fly ash
F – sample containing 20 mass% of fly ash

Acronyms

DSC – differential scanning calorimetry
DTA – differential thermal analysis
TGA – thermogravimetry analysis
TDA – thermodilatometric analysis

Greek symbols

λ – thermal conductivity, [$Wm^{-1}K^{-1}$]
ρ – density, [kgm^{-3}]
ρ_0 – initial density, [kgm^{-3}]

References

[1] Stubna, I., *et al.*, Mechanical Properties of Kaolin-Base Ceramics During Firing, *Processing,* Advances in Ceramics – Characterization, Raw Materials, Properties, Degradation and Healing (Ed. Costas Sikalidis), InTech, Rijeka, Croatia, 2011, pp. 229-244

[2] Chmelik, F., *et al.*, Creation of Microcracks in Porcelain During Firing, *Journal of the European Ceramics Society, 31* (2011), 13, pp. 2205-2209
[3] Norton, F. H., *Fine Ceramics – Technology and Application*, McGraw-Hill Book Co., New York, USA, 1970
[4] Kadir, A. A., Sarani, N. A., An Overview of Wastes Recycling in Fired Clay Bricks, *International Journal of Integrated Engineering, 4* (2012), 2, pp. 53-69
[5] Monteiro, S. N., Vieira, C. M. F., Effect of Oily Waste Addition to Clay Ceramic, *Ceramics International, 31* (2005), 2, pp. 353-358
[6] Pinheiro, R. M., *et al.*, Recycling of Waste from the Paper Production into Red Ceramic, *Materia, 13* (2008), 1, pp. 220-227
[7] Sokolar, R., Effect of Calcite on the Brick Body Closing, *Interceram, 59* (2010), 2, pp. 123-127
[8] Sokolar, R., *et al.*, Mechanical Properties of Ceramic Bodies Based on Calcite Waste, *Ceramics International, 38* (2012), 8, pp. 6607-6612
[9] Stubna, I., *et al.*, Elastic Properties of Waste Calcite-clay Ceramics During Firing, *Journal of the Ceramic Society of Japan, 120* (2012), 1405, pp. 351-354
[10] Monteiro, R. C. C., *et al.*, Mechanical Characteristics of Clay Structural Ceramics Containing Coal Fly Ash, *International Journal of Mechanics and Materials in Design, 4* (2008), 2, pp. 213-220
[11] Zimmer, A., Bergmann, C. P., Fly Ash of Mineral Coal as Ceramic Tiles Raw Material, *Waste Management, 27* (2007), 1, pp. 59-68
[12] Olgun, A., *et al.*, Development of Ceramics Tiles from Coal Fly Ash and Tincal Ore Waste, *Ceramics International, 31* (2005), 1, pp.153-158
[13] Ozsoy, E. A., *et al.*, Effect of Class C Fly Ash on Mechanical Properties of Clays, *Proceedings*, 10th ECerS Conference Goeller Verlag, Baden Baden, Germany, 2007, pp. 1606-1609
[14] Queralt, I., *et al.*, Use of Coal Fly Ash for Ceramics: A Case Study for a Large Spanish Power Station, *Fuel, 76* (1997), 8, pp. 787-789
[15] Sokolar, R., Vodova, L., The Effect of Fluidized Fly Ash on the Properties of Dry Pressed Ceramic Tiles Based on Fly Ash-clay Body, *Ceramics International, 37* (2011), 7, pp. 2879-2885
[16] Stubna, I., *et al.*, Simple Push-Rod Dilatometer for Dilatometry of Ceramics, *Proceedings,* Conference Research and Teaching of Physics on the Context of University Education, SPU, Nitra, Slovakia, 2007, pp. 69-74
[17] Zuda, L., Cerny, R., Measurement of Linear Thermal Expansion Coefficient of Alkali-activated Aluminosilicate Composites up to 1000 °C, *Cement & Concrete Composites, 31* (2009), 4, pp. 263-267
[18] Zeng, M., Shields, D. H., Nonlinear Thermal Expansion and Contraction of Asphalt Concrete, *Canadian Journal of Civil Engineering, 26* (1999), 1, pp. 26-34
[19] Trnik, A., *et al.*, Measurement of Linear Thermal Expansion Coefficient of Concrete at High Temperatures: A Comparison of Isothermal and Non-Isothermal Method, *Cement Wapno Beton, 17* (2012), 6, pp. 363-372
[20] Podoba, R., *et al.*, Upgrading of TGA/DTA Analyzer Derivatograph, *Epitoanyag, 64* (2012), 1-2, pp. 28-29
[21] Parker, W. J., *et al.*, Flash Method of Determining Thermal Diffusivity, Heat Capacity, and Thermal Conductivity, *Journal of Applied Physics, 32* (1961), 9, pp.1679-1684
[22] Vozar, L., *Flash Method for Thermal Diffusivity Measurement. Theory and Praxis*, CPU, Nitra, Slovakia, 2001
[23] ***, JCGM 100:2008, Evaluation of Measurement Data – Guide to the Expression of Uncertainty in Measurement, Joint Committee for Guides in Metrology, 2008
[24] ***, Guide to the Expression of Uncertainty of Measurement, Saudi Arabian Standards Organization, Rijad, 2006
[25] Kovac, J., Thermal Conductivity and Thermal Diffusivity of Ceramics Materials on Kaolin Base in Temperature Range 20-800 °C (in Slovak), Ph. D. thesis, CPU, Nitra, Slovakia, 2013
[26] Stubna, I., *et al.*, Measuring the Flexural Strength of Ceramics at Elevated Temperatures – An Uncertainty Analysis, *Measurement Science Review, 14* (2014), 1, pp. 35-40
[27] Stubna, I., *et al.*, Determination of Young's Modulus of Ceramics from Flexural Vibration at Elevated Temperatures, *Acta Acustica United with Acustica, 97* (2011), 1, pp. 1-7
[28] Hanykyr, V., Kutzendorfer, J., *Technology of Ceramics* (in Czech), Silkatovy Svaz, Praha, Czech Republic, 2008
[29] Gualtieri, A. F., Ferrari, S., Kinetics of Illite Dehydroxylation, *Physics and Chemistry of Minerals, 33* (2006), 7, pp. 490-501

[30] Hlavac, J., *Technology of Silicates* (in Czech), SNTL, Praha, Czech Republic, 1981
[31] Pospisil, Z., Koller, A., *Fine Ceramics, Basics of Technology* (in Czech), SNTL/ALFA, Praha, Czech Republic, 1981
[32] Ondruska, J., *et al.*, Degree of Conversion of Dehydroxylation in a Large Electroceramic Body, *International Journal of Thermophysics, 32* (2011), 3, pp. 729-735
[33] Stubna, I., Trnik, A., Young's Modulus of Porcelain Mixture After Firing in the Dehydroxylation Region, *Ceramics-Silikaty, 51* (2007), 2, pp.102-105
[34] Frost, R. L., *et al.*, Thermogravimetric Analysis of Selected Group (II) Carbonateminerals – Implication for the Geosequestration of Greenhouse Gases, *Journal of Thermal Analysis and Calorimetry, 95* (2009), 3, pp. 999-1005
[35] Rodriguez-Navarro, C., *et al.*, Thermal Decomposition of Calcite: Mechanisms of Formation and Textural Evolution of Cao Nanocrystals, *American Mineralogist, 94* (2009), 4, pp. 578-593

Paper submitted: September 11, 2013
Paper revised: June 18, 2014
Paper accepted: June 20, 2014